Synthesis and Structural Studies of Cationic Bis- and Tris(pyrazol-1-yl)methane Acyl and Methyl Complexes of Ruthenium(II): Localization of the Counterion in Solution by NOESY NMR Spectroscopy

Alceo Macchioni,*,† Gianfranco Bellachioma,† Giuseppe Cardaci,†
Gabriele Cruciani,† Elisabetta Foresti,‡ Piera Sabatino,‡ and Cristiano Zuccaccia†

*Dipartimento di Chimica, Università di Perugia, Via Elce di Sotto 8, 06123 Perugia, Italy,
and Dipartimento di Chimica "G. Ciamician", Università di Bologna, Via Selmi 2,
40126 Bologna, Italy*

Complex *fac*-Ru(PMe$_3$)(CO)$_3$(Me)I (**1**) reacts with tris- and bis(pyrazol-1-yl)methane, in the presence of NaBPh$_4$, affording *cis*-[Ru(PMe$_3$)(CO)$_2$(COMe)(η^2-pz$_3$-CH)]BPh$_4$ (**2**) and *cis*-[Ru(PMe$_3$)(CO)$_2$(COMe)(pz$_2$-CH$_2$)]BPh$_4$ (**4**), respectively. Complexes **2** and **4** decarbonylate leading to [Ru(PMe$_3$)(CO)(COMe)(η^3-pz$_3$-CH)]BPh$_4$ (**3**) and a mixture of three methyl stereoisomers of *cis*-[Ru(PMe$_3$)(CO)$_2$(Me)(pz$_2$-CH$_2$)]BPh$_4$ (**5**−**7**), respectively. The byproduct of the synthesis of **1**, *fac,cis*-Ru(PMe$_3$)(CO)$_3$(I)$_2$ (**8**), reacts with bis(pyrazol-1-yl)methane affording *cis*-[Ru(PMe$_3$)(CO)$_2$(I)(pz$_2$-CH$_2$)]BPh$_4$ (**9**). The stereochemistry of the complexes, the dynamic processes existing between them, and the interionic structures of all of the cationic complexes were investigated by the phase-sensitive ^{1}H NOESY NMR spectra in CD$_2$Cl$_2$. The solid-state crystal structure of **4**, obtained by single-crystal X-ray studies, was compared from the intramolecular and interionic point of views with that in solution with the help of 3-21G* ab initio and AMI−SM2 semiempirical quantum mechanical and docking mechanic calculations. In particular, the differences of interaction energy of the six solid-state ion pairs determined by the cation and the six symmetry-related anions surrounding it were estimated. The main result is that the averaged preferred position of the counterion in solution corresponds to the ion-pair electrostatically ($\Delta E_{el} > 2.5$ kcal/mol) and "sterically" ($\Delta E_{st} > 3.7$ kcal/mol) favored in the solid state.

Introduction

Cationic organometallic complexes have been increasingly used intensively in homogeneous catalysis. In particular, a noninnocent role is now attributed to the counterion in activating or preventing catalytic processes such as olefin polymerizations,[1] CO−olefin copolymerizations,[2] Diels−Alder reactions.[3] It is generally accepted that the counterion has to be large and weakly coordinating[4] in order to enhance the chemical reactivity of metal complexes and obtain a better catalyst. On the other hand, direct information concerning the coordinating capacity of the counterion and its specific inter-

actions with the organometallic moiety are difficult to obtain. This prompted us to search for a different approach to investigate organometallic ion pairs in solution based on NMR. We developed a method[5] that allows the determination of the interionic structures[6] of cationic organometallic complexes in solution based on the detection of interionic contacts, i.e., dipolar interactions between nuclei belonging to the counterion and to the organometallic moieties, in the NOESY or HOESY NMR spectra. The main result of this method is the possibility to understand which is the averaged position of the counterion with respect to the organometallic moiety. For compounds having the general formula *trans*-[M(PMe$_3$)$_2$(CO)(COMe)(N⌒N)]X (M = Fe

---

† Università di Perugia.
‡ Università di Bologna.
(1) (a) Chen, Y.-X.; Stern, C. L.; Marks, T. J. *J. Am. Chem. Soc.* **1997**, *119*, 2582. (b) Jia, L.; Yang, X.; Stern, C. L.; Marks, T. J. *Organometallics* **1997**, *16*, 842. (c) Chen, Y.-X.; Stern, C. L.; Yang, X.; Marks, T. J. *J. Am. Chem. Soc.* **1996**, *118*, 12451. (d) Yang, X.; Stern, C. L.; Marks, T. J. *J. Am. Chem. Soc.* **1994**, *116*, 10015.
(2) (a) Johnson, L. K.; Mecking, S.; Brookhart, M. *J. Am. Chem. Soc.* **1996**, *118*, 267. (b) Drent, E.; Budzelaar, P. H. M. *Chem. Rev.* **1996**, *96*, 663. (c) Milani, B.; Vicentini, L.; Sommazzi, A.; Garbassi, F.; Chiarparin, E.; Zangrando, E.; Mestroni, G. *J. Chem. Soc., Dalton Trans.* **1996**, 3139.
(3) (a) Evans, D. A.; Murry, J. A.; von Matt, P.; Norcross, R. D.; Miller, S. J. *Angew. Chem., Int. Ed. Engl.* **1995**, *34*, 798. (b) Carmona, D.; Cativiela; C.; Garcia-Correas, R.; Lahoz, F. J.; Lamata, M. P.; Lopez, J. A.; Lopez-Ram de Viu, M. P.; Oro, L. A.; San José, E.; Viguri, F. *Chem. Commun.* **1996**, 1247.
(4) Strauss, S. H. *Chem. Rev.* **1993**, *93*, 927.

(5) (a) Bellachioma, G.; Cardaci, G.; Macchioni, A.; Reichenbach, G.; Terenzi, S. *Organometallics* **1996**, *15*, 4349. (b) Macchioni, A.; Bellachioma, G.; Cardaci, G.; Gramlich, V.; Rüegger, H.; Terenzi, S.; Venanzi, L. M. *Organometallics* **1997**, *16*, 2139.
(6) For references on interionic studies of organic salts which catalyze phase-transfer reactions see: (a) Pochapsky, T. C.; Wang, A.-P.; Stone, P. M. *J. Am. Chem. Soc.* **1993**, *115*, 11084. (b) Pochapsky, T. C.; Stone, P. M. *J. Am. Chem. Soc.* **1990**, *112*, 6714. (c) Pochapsky, T. C.; Stone, P. M. *J. Am. Chem. Soc.* **1991**, *113*, 1460. For references on interionc studies of organolithium ion pairs, see: (d) Hoffman, D.; Bauer, W.; Schleyer, P. v. R. *J. Chem Soc., Chem. Commun.* **1990**, 208. (e) Bauer, W.; Müller, G.; Pi, R.; Schleyer, P. v. R. *Angew. Chem., Int. Ed. Engl.* **1986**, *25*, 1103. (f) Bauer, W.; Klusener, P. A. A.; Harder, S.; Kanters, J. A.; Duisenberg, A. J. M.; Brandsma, L.; Schleyer, P. v. R. *Organometallics* **1988**, *7*, 552. (g) Bauer, W.; Clark, T.; Schleyer, P. v. R. *J. Am. Chem. Soc.* **1987**, *109*, 970. (h) Bauer, W.; Feigel, M.; Müller, G.; Schleyer, P. v. R. *J. Am. Chem. Soc.* **1988**, *110*, 6033.
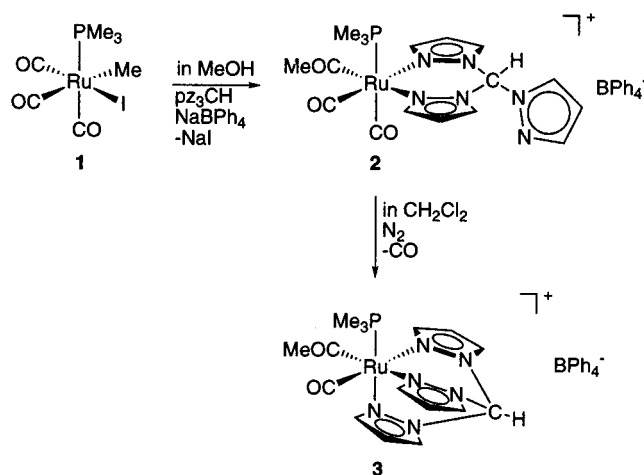
Chart 1
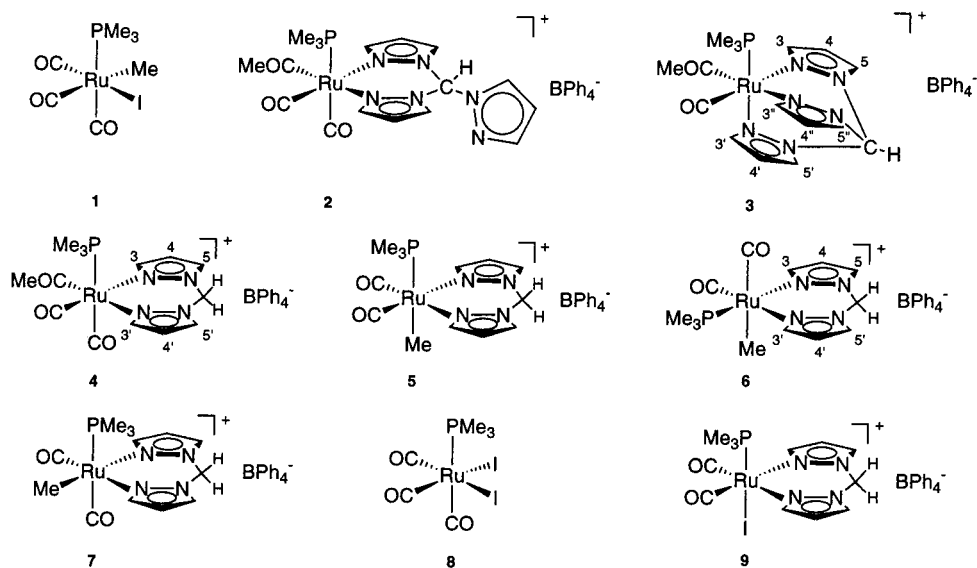
and Ru), we found that the counterion interacts in methylene chloride specifically with protons belonging to the N⌒N ligands and to the PMe₃ groups. In no case were there contacts between the NMR-active nuclei of the counterion and the COMe protons. These observations were done both for "organic" counterions (X = BPh₄) and "inorganic" counterions (X = BF₄). It is evident that the specific averaged position of the counterions cannot be explained on the basis of only a maximization of the van der Waals interactions but must also involve an electrostatic gain.

In this paper, we report the synthesis of other new cationic compounds, shown in Chart 1, derived from the reaction of *fac*-Ru(PMe₃)(CO)₃(Me)I[7] (**1**) with bis- and tris(pyrazol-1-yl)methane ligands. Different from the above-mentioned compounds, the acyl compounds decarbonylate affording a mixture of methyl complexes that are in slow equilibrium in solution compared to the NMR time scale. The phase-sensitive ¹H NOESY NMR spectra allows the dynamical processes, the stereochemistry of the various stereoismers, and the more interesting interionic structures of the cationic complexes to be investigated. A comparison between the solid-state structure of complex **4** (obtained by X-ray single-crystal studies) and that in solution carried out with the help of semiempirical and ab initio quantum mechanical and mechanical calculations is also reported. The semiempirical and ab initio quantum mechanical calculations allowed us to evaluate the electron density on both ionic fragments. The mechanic calculations led to the energy interaction values of six ion pairs determined by the six symmetry-related anions surrounding the cation in the solid state.

Results and Discussion

Synthesis. The oxidative addition of MeI on Ru-(PMe₃)(CO)₄ affords a mixture of acyl complexes that easily decarbonylate by bubbling N₂ in the solution leading to the methyl complex **1** that is unstable in

(7) (a) Reichenbach, G.; Cardaci, G.; Bellachioma, G.; *J. Chem. Soc., Dalton Trans.*, **1982**, 847. (b) Bellachioma, G.; Cardaci, G.; Macchioni, A.; Madami A. *Inorg. Chem.* **1993**, *32*, 554.

Scheme 1

solution.[7] Even in the solid state, it slowly decomposes and is usually stored as a mixture of acyl complexes under CO atmosphere.

Complex **1** can easily ionizise the Ru–I bond. It also undergoes methyl migration on a cis CO and dissociation of a Ru–CO bond. A maximum of three coordination sites can be potentially left free.

The reaction of complex **1** with pz₃-CH (pz = pyrazol-1-yl ring) in the presence of NaBPh₄ affords the acyl η²-complex **2**, according to Scheme 1, where one of the pz rings remains uncoordinated.
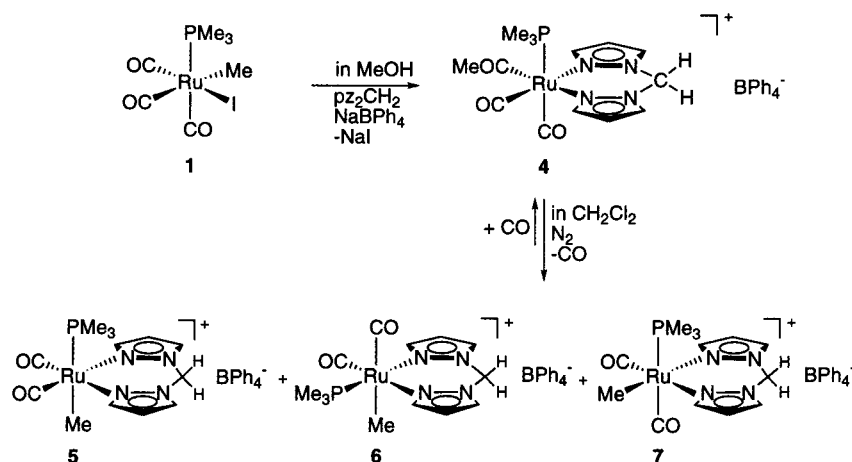
By dissolving complex **2** in CH₂Cl₂ and bubbling in the solution N₂, it is possible to allow the coordination of the third pyrazolyl ring, forming the η³-complex **3**. Complex **3** is a very stable complex that is not sensitive to moisture, does not react with CO to give back complex **2**, and does not undergo further decarbonylation.

The reaction of complex **1** with pz₂-CH₂ in the presence of NaBPh₄ affords only one acyl complex (**4**) (see Scheme 2) whose stereochemistry in solution and in the solid state has been clarified by ¹H NOESY NMR spectroscopy and X-ray single-crystal studies, respectively (see below).

Complex **4** is also insensitive to moisture but in CH₂-Cl₂ solution it undergoes spontaneous decarbonylation

Scheme 2

reaching an equilibrium with a mixture of three methyl complexes **5**−**7** in the ratio 1:1.6:0.1 at 25 °C. By warming the solution to 38 °C, the equilibrium is completely shifted toward the methyl complexes. Complexes **5**−**7** equilibrate in solution, and any attempt to separate them was unsuccessful. The stereochemistry of complexes **5**−**7** has been clarified by ^{1}H NOESY NMR spectroscopy (see below). The acyl complex **4** is regained by dissolving the methyl mixture in CH_2Cl_2 under CO atmosphere for 2 h.

Both the coordination of the third pyrazolyl ring in the case of the reaction of **1** with pz$_3$-CH and the possibility to decarbonylate complex **4** to obtain the methyl complexes **5**−**7** derive from the lower electron density on ruthenium complexes respect to the analogous ones deriving from *trans*-Ru(PMe$_3$)$_2$(CO)$_2$(Me)I[5b] due to the presence in complex **1** of only one phosphine. This weakens the Ru−CO bond and allows the decarbonylation.

One of the byproduct of the oxidative addition of MeI to complex **1** is complex **8** that can react with pz$_2$-CH$_2$ in the presence of NaBPh$_4$ affording complex **9** owing to the ionization of one Ru−I bond and dissociation of a Ru−CO bond.

Characterization and Structure. (a) Solutions. Intramolecular Structure. Characterization of complexes **2**−**9** in this phase was carried out with IR and ^{1}H, ^{13}C, and ^{31}P NMR spectroscopies.

The IR spectra of complexes show bands in the carbonyl region between 2080−1940 and 1645−1600 cm^{-1}, relative to the CO and COMe stretchings, respectively. When complexes contain two carbonyl groups (**2**, **4**−**7**, and **9**), we observe two stretching bands having similar intensity. This ensures that the two carbonyl groups are in the relative cis position.

The characterization of complex **2** is not complete because, in solution, it transforms into complex **3**. In complex **3**, all three pyrazolyl rings are nonequivalent owing to the different trans substituents. Consequently, there are nine resonances both in the ^{1}H and the ^{13}C NMR spectra. The assignment of the H-3 protons, which fall at higher frequency, is easily done by the ^{1}H NOESY NMR spectrum considering that only the H-3′ (7.89 ppm) (for numeration see Chart 1) does not show any contact with the protons of the phosphine and must belong to the pyrazolyl ring trans to PMe$_3$. Furthermore, only the resonance at 8.41 ppm shows contacts with the protons of the phosphine and of the COMe group and must be H-3. The remaining resonance at 7.62 ppm is due to H-3″. The other protons of the rings are assigned by the "intraring" contacts.

The stereochemistry of complex **4** derives from the observation in the ^{1}H NOESY NMR spectrum of two "contacts" between both H-3 and H-3′ protons and the protons of PMe$_3$ that ensure that the two pyrazolyl rings are both in the relative cis position with respect to PMe$_3$. Furthermore, the fact that they are not equivalent leads to the stereochemistry reported in Chart 1.

The stereochemistry of the methyl complexes **5** is straightforward obtained because of the equivalence of the two pyrazolyl rings. The stereochemistry of complex **6** is derived from considerations similar to the previous ones. In fact, one of the H-3 shows a contact only with the protons of Me, while H-3′ shows contacts with the protons of Me and of PMe$_3$. The only possible structure is reported in Chart 1. The determination of the third methyl complex **7** having very low concentration can also be done considering that it is the only other possible one having the two CH$_2$ protons inequivalent.

The two protons of the CH$_2$ groups in complexes **4**−**7** and **9** are inequivalent and their assignment is done based on the presence of contacts with the protons of the apical groups. The frequencies of resonance of these protons are relatively low (4.5−5.5 ppm) indicating a shielding of the aromatic groups of the tetraphenylborate.[4a] This is confirmed by the interionic contacts.

It is interesting to notice that the phase-sensitive ^{1}H NOESY spectrum of the methyl mixture shows some cross-peaks with the same sign of the diagonal indicating the presence of exchange processes. In particular, there are exchange cross-peaks between (a) the methyl groups belonging to the two methyl complexes **5** and **6**; (b) the H-3 belonging to the two methyl stereoisomers **5** and **6**; and (c) the methyl group of complex **6** with the COMe group of **4** present in very low quantity. These observations are explainable only by assuming the formation of one or more unsaturated intermediates.

The assignment of carbon resonances was carried out in some cases by ^{1}H,^{13}C inverse correlation experiments with gradients or considering that the order of resonances in ^{13}C is the same as in ^{1}H spectra.

Interionic Structures. The interionic structures of complexes **3**−**6** and **9** were investigated in CD$_2$Cl$_2$ by the phase-sensitive ^{1}H NOESY NMR spectra by detect-
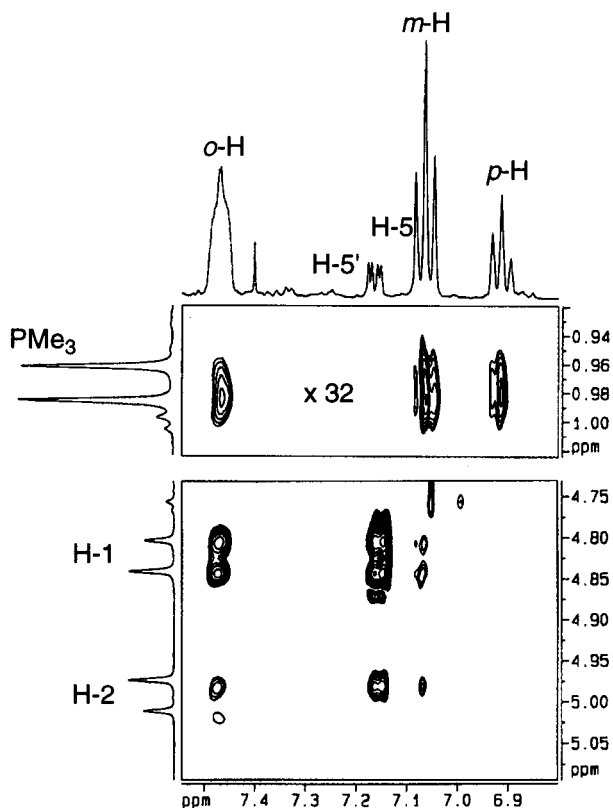
Figure 1. Two sections of ^{1}H NOESY spectrum of compound **4**, recorded at 400.13 MHz in CD_2Cl_2, showing the interionic contacts between the PMe_3 group and *o*-H, *m*-H, and *p*-H protons, and between CH_2 and *o*-H protons.

ing contacts between protons belonging to the BPh_4^- and those of the organometallic moieties. The information derived from the detection of nuclear dipolar interactions in solution allows the determination of the averaged interionic structures.

Complex **3** shows interionic contacts between the H-5 protons and the *o*-H (strong) and between the protons of the PMe_3 group and the *m*-H (weak). In complex **4** there are interionic contacts between CH_2 and PMe_3 (weak) protons and *o*-H, *m*-H, and *p*-H (see Figure 1). The intensity of cross-peaks of the section relative to PMe_3 groups in Figure 1 have been multiplied 32 times. Complex **5** shows interionic contacts between the PMe_3 protons and the *m*-H and *p*-H and between the H-5 protons and the *o*-H. Complex **6** shows only interionic contacts between H-5 protons and *o*-H and *m*-H. Complex **9** shows interionic contacts between the PMe_3 protons and the *m*-H and *p*-H. Furthermore, a selective interionic contact between H-1 and *o*-H protons has been observed (see Figure 2). In general, in all complexes, there is a preferential interaction between the more shielded H-1 and *o*-H protons. Also, the intramolecular contact H-5−H-1 is stronger than H-5−H-2 that is not visible in Figure 2. These findings are perfectly explainable considering that H-1, which points toward one phenyl ring of BPh_4^-, is also closer to H-5 than H-2 (see scheme inside Figure 2).

From the above observations, one can deduce as a general consideration that in all cases the counterion spends most of its time close to the pyrazolyl rings, in agreement with previous results.[5] Furthermore, in complexes **3**−**5**, the counterion is shifted toward the
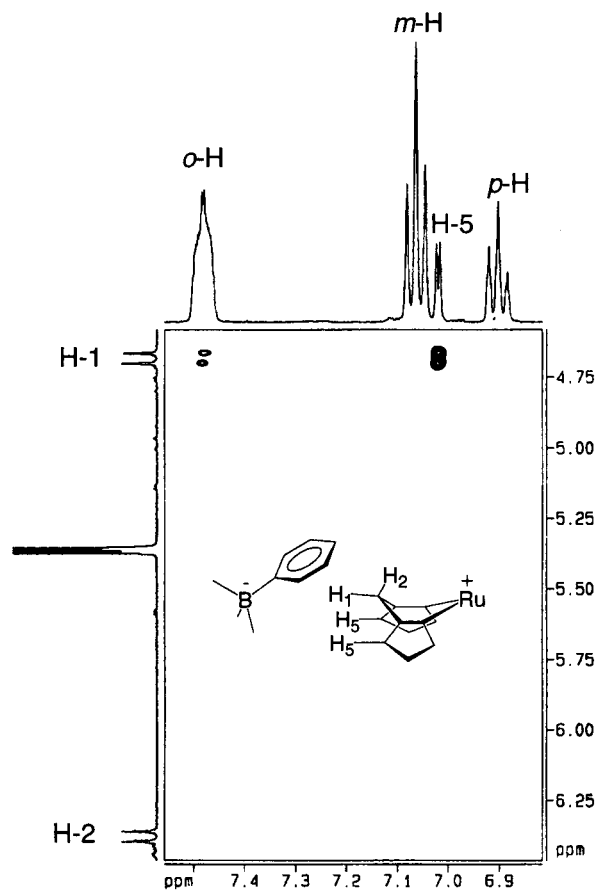

Figure 2. Section of ^{1}H NOESY spectrum of compound **9**, recorded at 400.13 MHz in CD_2Cl_2, showing the specific interionic contact between the H-1 and *o*-H, and intramolecular contact between H-1 and H-5.
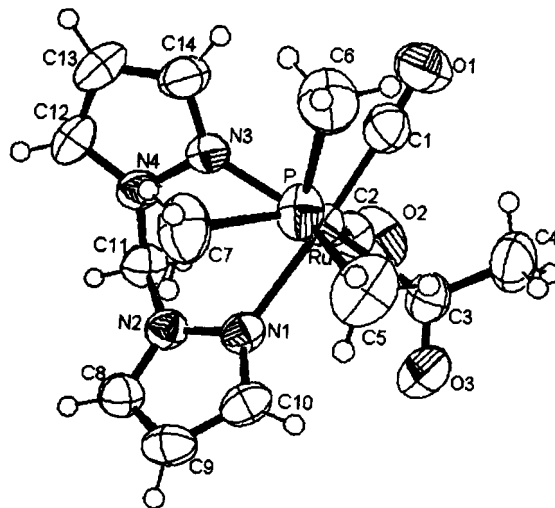

Figure 3. An ORTEP view of cationic fragment of **4**.

phosphine group, while in complex **6** it stays in front of the face determined by the pyrazolyl rings and the CO trans to Me. In none of the spectra are there contacts between the protons of the tetraphenylborate counterion and the Me and COMe groups.

(b) Crystal and Molecular Structure of Cation 4 As Its BPh_4^- Salt. The overall molecular geometry of cation **4** is shown in Figure 3; Table 1 reports selected bond distances and angles. The coordination geometry at the metal center is approximately octahedral, with mutually cis carbonyl ligands and an equatorial plane

Table 1. Selected Bond Lengths (Å) and Bond Angles (deg) for 4

Bond Lengths (Å)

Ru−C(1)	1.858(7)	N(3)−N(4)	1.351(6)
Ru−C(2)	1.921(6)	N(4)−C(12)	1.351(7)
Ru−C(3)	2.056(6)	N(4)−C(11)	1.430(7)
Ru−N(1)	2.190(5)	O(1)−C(1)	1.131(8)
Ru−N(3)	2.233(5)	O(2)−C(2)	1.125(7)
Ru−P	2.401(2)	O(3)−C(3)	1.222(8)
N(1)−C(10)	1.331(7)	C(3)−C(4)	1.488(9)
N(1)−N(2)	1.337(6)	C(8)−C(9)	1.350(8)
N(2)−C(8)	1.346(7)	C(9)−C(10)	1.374(9)
N(2)−C(11)	1.442(7)	C(12)−C(13)	1.345(9)
N(3)−C(14)	1.333(7)	C(13)−C(14)	1.368(9)

Bond Angles (deg)

C(1)−Ru−C(2)	86.8(3)	C(2)−Ru−P	173.5(2)
C(1)−Ru−C(3)	92.5(3)	C(3)−Ru−P	90.4(2)
C(2)−Ru−C(3)	84.1(3)	N(1)−Ru−P	87.02(12)
C(1)−Ru−N(1)	175.5(2)	N(3)−Ru−P	87.46(14)
C(2)−Ru−N(1)	96.5(2)	N(2)−N(1)−Ru	122.3(3)
C(3)−Ru−N(1)	90.9(2)	N(1)−N(2)−C(11)	120.9(5)
C(1)−Ru−N(3)	91.0(2)	N(4)−N(3)−Ru	121.6(3)
C(2)−Ru−N(3)	98.2(2)	N(3)−N(4)−C(11)	119.2(5)
C(3)−Ru−N(3)	176.0(2)	O(1)−C(1)−Ru	178.1(6)
N(1)−Ru−N(3)	85.6(2)	O(2)−C(2)−Ru	170.4(6)
C(1)−Ru−P	90.1(2)		

Table 2. Symmetry Operations Relating Anions

(i)	$1 - x$	$-y$	$-z$
(ii)	x	$1 + y$	z
(iii)	x	$\Omega - y$	$\Omega + z$
(iv)	x	$-\Omega - y$	$\Omega + z$
(v)	$2 - x$	$-y$	$-z$

Figure 4. A ball and stick representation of the ionic pair where the notably shortest Ru···B metal contact is found.

defined by the bis-pyrazolyl ligand, the acyl group, and one carbonyl. The axial sites are occupied by the second CO and the phosphine ligands. The cation is clearly chiral, but the crystal contains the racemic mixture. The phosphine ligand is slightly bent toward the bis-pyrazolyl moiety (P−Ru−N1 87.0(1)° and P−Ru−N3 87.5-(1)°) while the trans carbonyl ligand bends away from it (C2−Ru−N3 98.2(2)°, C2−Ru−N1 96.5(2)° and C2−Ru−C3 83.9°). The P−Ru−C(2) angle is 173.5(2)°.

The two Ru−N bond distances (2.190(5) and 2.233(5) Å for Ru−N(1) and Ru−N(3), respectively) are slightly shorter than those reported[5b] for the parent species *trans*-[Ru(PMe₃)₂(CO)(COMe)(pz₂-CH₂)]BPh₄ (2.218(15) and 2.257(14) Å) and, like the latter, are significantly different, with the longer distance always trans to the better donor acyl ligand. The two pyrazolyl rings show complete planarity in each ring but are not coplanar (dihedral angle between the normals to the two planes 55°). The six-membered metallacycle containing the four nitrogen atoms adopts a half-chair conformation with the C(11) atom out of the least-squares plane through the remaining five of 0.79 Å and oriented on the side of the least hindering axial CO ligand.

Of the three Ru−C bond lengths, that relative to the acyl group, 2.056(6) Å, is strictly comparable to that found in the above-mentioned *trans*-[Ru(PMe₃)₂(CO)-(COMe)(pz₂-CH₂)]BPh₄, (2.055 Å), while the two metal−C₍carbonyl₎ distances are quite dissimilar (1.858(7) and 1.921(6) Å for Ru−C(1) and Ru−C(2), respectively), reflecting the different electronic configurations of the relative trans ligands. The longer Ru−C₍acyl₎ distance compared with Ru−C₍carbonyl₎ is primarily due to the fact that the CO ligands interact with two sets of π orbitals. The plane defined by the acyl ligand is almost coincident with the equatorial coordination plane (dihedral angle 14°), giving evidence of a delocalized Ru−C(3)−O(3) π bond.

Finally, the Ru−P distance, 2.403 Å, trans to a carbonyl group is longer than those found in the above-mentioned parent species, where the two phosphine groups are trans to each other.
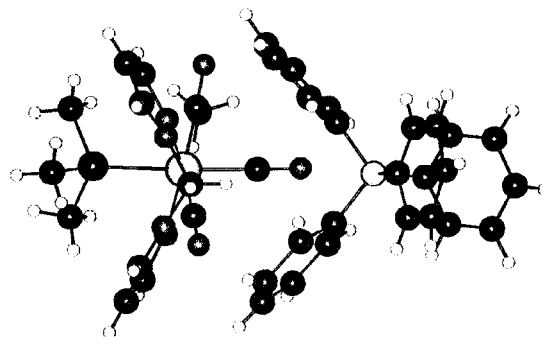
The counterion, BPh₄⁻, orients two of its phenyl groups almost parallel to the two pyrazolyl rings (angles between the normals to the planes passing through C(15) to C(20) with pz(2) (N(3) to C(14)) and C(21) to C(26) with pz(1) (N(1) to C(10)) of 19° and 15°, respectively.

Hydrogen bond interactions are found exclusively within the cations, one intramolecular C(10)−H(10)···O3 and one intermolecular one C(4)−H(4)···O(3) (symmetry operator 1−*x*, 1−*y*, −*z*) with D···A distances of 2.94 and 3.49 Å, respectively, and D−H···A angles of 115° and 154°.

Solid State versus Solution Interionic Structure of Complex 4. Since the main interest in the structure was focused on the H···H interionic contacts, we have calculated, in the solid state, a 3.5 Å coordination sphere around each hydrogen atom. This way, we have evidenced the six symmetry-related anions surrounding the cation and giving the closest contacts with it; the relative symmetry operations are shown in Table 2.

It is interesting to note that strong interionic contacts (starting from 2.45 Å) between the PMe₃ moiety in the cation and the *o-, m-,* and *p*-H atoms of the BPh₄⁻ phenyl groups, already observed in solution, are kept in the solid state. Analogously, the CH₂ protons in C(11) are also involved in contacts with anionic *o-* and *m*-H atoms. In addition, in contrast to what was observed in solution, in the solid state the acyl protons are also involved in interactions with *o-* and *m*-H atoms, while the protons of the pyrazolyl rings interact with *o-, m-,* and *p*-H atoms with distances for both kind of contacts ranging from 2.55 to 3.49 Å. In conclusion, considering the six pairs, all of the moieties of the cation bearing protons are close enough to interact with the protons of at least one anion (distances < 3.5−4 Å) in the solid state.

It must be underlined that the ionic pair where the notably shortest Ru···B metal contact is found (6.71 vs 8.39 Å av), i.e., the closest packed pair that was chosen as the crystallographic asymmetric unit exhibits few and quite long H···H contacts because of the almost parallel orientation of two phenyl rings with respect to the pyrazolyl rings as reported above (Figure 4).
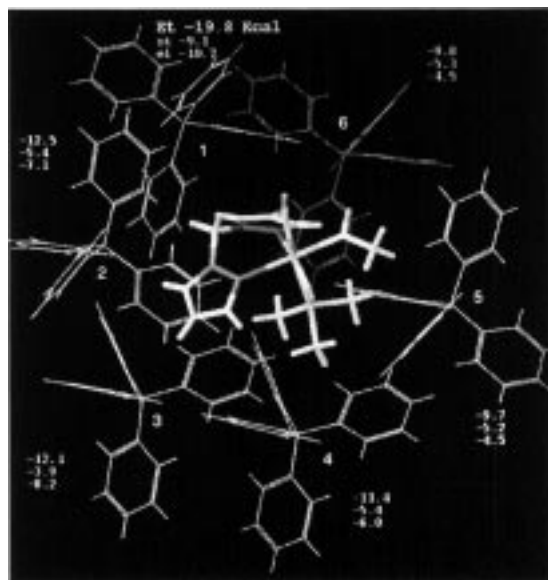
Figure 5. A schematization of the six symmetry-related anions surrounding the cation.

Table 3. Relative Electrostatic (ΔE_{el})[a] and Steric (ΔE_{st})[a] Energy of the Cation-Anion Interactions for All Six Possible Pairs Calculated by the DOCK Method Implemented in SYBYL[12]

pair	ΔE_{el} (kcal/mol)	ΔE_{st} (kcal/mol)	ΔE_{tot} (kcal/mol)
1	0	0	0
2	3.6	3.7	7.3
3	2.5	5.2	7.7
4	4.7	3.7	8.4
5	6.2	3.9	10.1
6	6.2	3.8	10.0

[a] The pair 1 cation that is the most stable is taken as reference, and ΔE values are calculated as $E_x - E_1$ and are, consequently, all positive.

In a methylene chloride solution and at our concentrations, it is known that organometallic complexes are principally present as tight ion pairs. We wondered if one of the six pairs selected in the solid state is the energetically favored ion pair and if this one is that we found in solution. For this reason, crystallographic coordinates of the above-mentioned six cation–anion pairs have been used as input for a calculation of the sterical and electrostatic energy involved in ion-pair interactions (Figure 5, Table 3). We first calculated the charge distribution in separated fragments. Interestingly, from the 3-21G* ab initio and AMI–SM2 semiempirical calculations, we obtained that the positive charge is not centered on Ru but is mainly delocalized on the bispyrazolylmethane ligand. This means that the already favored counterion–cation interaction on the side of the pyrazolyl rings from the van der Waals point of view is reinforced by a stronger electrostatic interaction. It is now easier to understand why also completely inorganic counterions (such as BF_4^-), where we can assume that the electrostatic interactions are more important, stay in the same position, in front of the pyrazolyl rings.[5b] Another interesting point is that the oxygen of the acyl group comes out partially negatively charged. There should be repulsion between this oxygen and the counterion. This agrees perfectly with the fact that we never observed interionic contacts between the COMe protons and NMR active nuclei of the counterions.

The estimation of the electrostatic and "steric" energy of the cation–anion interaction for all six possible pairs was calculated by docking mechanic calculations. The numerical data are reported in Table 3. As a general trend, the counterion prefers to stay close to the "more organic" side of the molecule, i.e., close to the pyrazolyl rings. Furthermore, there is indeed a cation–ion pair (**1** in Figure 5) that is more stabilized than the others both from the electrostatic and steric points of view ($\Delta E > 7.3$ kcal/mol, $\Delta E_{el} > 2.5$ kcal/mol, $\Delta E_{st} > 3.7$ kcal/mol). This is the pair chosen as the crystallographic asymmetric unit reported in Figure 4 and is the principal ion pair that we find in solution. It must be said that in solution we also observed a weak interionic contact between PMe$_3$ protons and *o*-H, *m*-H, and *p*-H that is not justified simply considering the pair shown in Figure 4. Of course, several dynamic processes are active in solution that we cannot consider from the simplistic assumption that one solid-state pair is strictly conserved in solution. For example, an inversion of the six-member metallacycle containing the four nitrogen atoms is enough to allow the contacts between BPh_4^- and PMe$_3$ protons. In any case, as a first approximation, we can assume that dissolving the salt in methylene chloride allows the solvent to electronically decouple the cation from all but one anion. This last anion is the one that interacts more strongly with the cation in the solid state.

Conclusions

Intramolecular and interionic structural studies in solution on new acyl and methyl compounds **2–9** have been performed by ^{1}H NOESY NMR spectroscopy. In particular, for compound **4**, the interionic structure in solution was compared with that in the solid state with the help of quantum mechanical and mechanic calculations. 3-21G* ab initio and AMI–SM2 semiempirical quantum mechanical calculations indicated that there is a partial positive charge delocalized on the pyrazolyl rings and a partial negative charge accumulated on the oxygen atom of COMe group. By using such a charge distribution, the energy interaction values of six ion pairs determined by the six symmetry-related anions surrounding the cation in the solid state have been calculated using the DOCK method implemented in SYBYL. The ion pair where the counterion stays in front of the bis-pyrazolyl rings (shown in Figure 4) is favored in the solid state both from the electrostatic ($\Delta E_{el} > 2.5$ kcal/mol) and steric ($\Delta E_{st} > 3.7$ kcal/mol) points of view. This is the principal ion pair found in solution based on the detection of interionic contacts in the ^{1}H NOESY NMR spectra. This means that, in the case of a weak coordinating solvent such as methylene chloride, the dissolution process corresponds to an electronically decoupling of the cation from all but the most stabilized anion in the lattice.

Experimental Section

General Data. Complex **1** was prepared according to the literature.[7] Reactions were carried out in a dried apparatus under a dry inert atmosphere of nitrogen using standard

Schlenk techniques. Solvents were purified prior to use by conventional methods.[8] pz$_2$-CH$_2$ and pz$_3$-CH ligands were synthesized according to the literature.[9] Pyrazole was purchased by Fluka and utilized without further purification.

IR spectra were taken on a 1725 X FTIR Perkin-Elmer spectrophotometer. One and two-dimensional ^{1}H, ^{13}C, and ^{31}P NMR spectra were measured on Bruker AC 200, DRX 400, and DRX 500 spectrometers. Referencing is relative to TMS and external 85% H$_3$PO$_4$. NMR samples were prepared dissolving about 20 mg of compound in 0.5 mL of CD$_2$Cl$_2$ bubling for 5 min with dried nitrogen. Two-dimensional ^{1}H NOESY NMR spectra, with a mixing time 800 ms, were measured as previously described.[10]

Preparation of *cis*-[Ru(PMe$_3$)(CO)(COMe)(η^3-pz$_3$-CH)]-BPh$_4$ (3). Complex **1** (100 mg, 0.32 mmol) and pz$_3$-CH (62 mg, 0.29 mmol) were dissolved in 5 mL of CH$_3$OH. NaBPh$_4$ (large excess) was added, and a white solid precipitated. The IR spectrum of the solid showed the presence of complexes *cis*-[Ru(PMe$_3$)(CO)$_2$(COMe)(η^2-pz$_3$-CH)]BPh$_4$ (**2**) and *cis*-[Ru(PMe$_3$)(CO)(COMe)(η^3-pz$_3$-CH)]BPh$_4$ (**3**). The solid was dissolved in CH$_2$Cl$_2$ (5 mL) and stirred at 35 °C for 2 h, obtaining only the η^3-complex **3**. The solvent was removed by bubbling N$_2$ in an open Schlenck flask, and the residual solid was washed with cold CH$_3$OH, dried, and crystallized from CH$_2$Cl$_2$/*n*-hexane (yield ca. 60%). Spectroscopic chracterization of complex **2**: ^{1}H NMR (CD$_2$Cl$_2$, 298 K) 8.36 (d, $^3J_{HH}$ = 2.2, H-3), 8.04 (d, $^3J_{HH}$ = 2.2, H-3′), 8.41 (d, $^3J_{HH}$ = 2.2, H-3″), 6.38 (t, $^3J_{HH}$ = 2.6, H-4), 6.35 (t, $^3J_{HH}$ = 2.6, H-4′), 6.32 (t, $^3J_{HH}$ = 2.6, H-4″), 2.49 (s, COMe), 0.96 (d, $^2J_{PH}$ = 9.7, PMe$_3$); ^{13}C{^{1}H} NMR 207.6 (s, CO), 164.2 (q, $^1J_{BC}$ = 48.6, C-ipso), 146.8 (s, C-3 or C-3′ or C-3″), 146.6 (s, C-3 or C-3′ or C-3″), 136.6 (s, *o*-C), 126.6 (s, *m*-C), 123.0 (s, *p*-C), 134.5 (s, C-5 or C-5′ or C-5″), 133.7 (s, C-5 or C-5′ or C-5″), 133.3 (s, C-5 or C-5′ or C-5″), 109.1 (s, C-4 or C-4′ or C-4″), 108.7 (s, C-4 or C-4′ or C-4″), 108.3 (s, C-4 or C-4′ or C-4″), 50.6 (s, CO*C*H$_3$), 17.4 (d, $^2J_{CP}$ = 33.1, PMe$_3$); ^{31}P{^{1}H} NMR −3.18; IR (CH$_2$Cl$_2$) ν_{CO} 2071, 1994, ν_{COMe} 1638 cm^{-1}. Characterization of complex **3**: ^{1}H NMR (CD$_2$Cl$_2$, 298 K) 8.41 (d, $^3J_{HH}$ = 2.2, H-3), 7.89 (d, $^3J_{HH}$ = 1.7, H-3′), 7.62 (d, $^3J_{HH}$ = 2.0, H-3″), 7.42 (m, *o*-H), 7.24 (d, $^3J_{HH}$ = 2.4, H-5), 7.21 (d, $^3J_{HH}$ = 2.8, H-5′), 7.20 (d, $^3J_{HH}$ = 2.7, H-5″), 7.06 (t, $^3J_{HH}$ = 7.3, *m*-H), 7.03 (s, C), 6.94 (t, $^3J_{HH}$ = 7.2, *p*-H), 6.37 (td, $^3J_{HH}$ = 2.5, H-4), 6.30 (m, H-4′ and H-4″), 2.51 (s, COMe), 1.43 (d, $^2J_{PH}$ = 9.8, PMe$_3$); ^{13}C{^{1}H} NMR 256.4 (d, $^2J_{CP}$ = 12.5, *C*OMe), 203.6 (d, $^2J_{CP}$ = 19.2, CO), 164.2 (q, $^1J_{BC}$ = 48.6, C-ipso), 147.5 (s, C-3), 146.4 (s, C-3′), 146.2 (s, C-3″), 136.6 (s, *o*-C), 126.6 (s, *m*-C), 123.0 (s, *p*-C), 134.8 (s, C-5), 134.3 (s, C-5′), 133.9 (s, C-5″), 109.0 (s, C-4′ and C-4″), 108.4 (s, C-4), 76.7 (s, CH), 47.2 (s, CO*C*H$_3$), 17.2 (d, $^2J_{CP}$ = 33.4, PMe$_3$); ^{31}P{^{1}H} NMR 15.62 (s); IR (CH$_2$Cl$_2$) ν_{CO} 1959, ν_{COMe} 1608 cm^{-1}. Anal. Calcd (found) for (C$_{40}$H$_{42}$N$_6$BO$_2$PRu): H, 5.45 (5.40); C, 60.80 (60.61); N, 10.71 (10.38).

Preparation of *cis*-[Ru(PMe$_3$)(CO)$_2$(COMe)(pz$_2$-CH$_2$)]-BPh$_4$ (4). Complex **1** (151 mg, 0.37 mmol) and pz$_2$-CH$_2$ (66 mg, 0.46 mmol) were dissolved in 5 mL of CH$_3$OH. NaBPh$_4$ (large excess) was added while CO was bubbled in the solution. Immediately a white solid precipitated. The solution was stirred for 30 min and put in the refrigerator at −18 °C for 12 h to complete the precipitation. The solid was filtered, washed with cold CH$_3$OH, dried, and crystallized from CH$_2$Cl$_2$/*n*-hexane (yield ca. 60%). Anal. Calcd (found) for (C$_{38}$H$_{40}$N$_4$BO$_3$PRu): H, 5.39 (5.42); C, 61.05 (60.86); N, 7.47 (7.50). Data for **4**: ^{1}H NMR (CD$_2$Cl$_2$, 298 K) 8.48 (d, $^3J_{HH}$ = 2.2, H-3), 7.56

(d, $^3J_{HH}$ = 2.1, H-3′), 7.42 (m, *o*-H), 7.04 (H-5′), 7.02 (t, $^3J_{HH}$ = 7.4, *m*-H), 7.01 (H-5), 6.87 (t, $^3J_{HH}$ = 7.2, *p*-H), 6.40 (td, $^3J_{HH}$ = 2.5, H-4), 6.36 (t, $^3J_{HH}$ = 2.5, H-4′), 4.93 (d, $^2J_{HH}$ = 15, H-2), 4.67 (d, $^2J_{HH}$ = 15, H-1), 2.61 (s, COMe), 0.95 (d, $^2J_{PH}$ = 9.6, PMe$_3$); ^{13}C{^{1}H} NMR 243.4 (d, $^2J_{CP}$ = 9.7, *C*OMe), 199.1 (d, $^2J_{CP}$ = 16.2, CO (cis)), 189.8 (d, $^2J_{CP}$ = 94.9, CO (trans)), 164.3 (q, $^1J_{BC}$ = , C-ipso), 147.8 (s, C-3), 146.1 (s, C-3′), 137.5 (s, C-5), 136.4 (s, *o*-C), 135.8 (s, C-5′), 126.4 (s, *m*-C), 122.6 (s, *p*-C), 108.9 (s, C-4′), 108.2 (s, C-4), 62.1 (s, CH$_2$), 51.9 (s, CO*C*H$_3$), 13.7 (d, $^2J_{CP}$ = 30.3, PMe$_3$); ^{31}P{^{1}H} NMR −3.31(s); IR (CH$_2$-Cl$_2$) ν_{CO} 2063, 1994, ν_{COMe} 1641 cm^{-1}.

Decarbonylation of Complex 4. Complex **4** (100 mg) was fluxed with N$_2$ at 35 °C in CH$_2$Cl$_2$ (3 mL) for 3h. The methyl complexes **5**−**7** were obtained quantitatively by adding *n*-hexane to the solution. Anal. Calcd. (found) for (C$_{37}$H$_{40}$N$_4$-BO$_2$PRu): H, 5.61 (5.63); C, 61.81 (61.47); N, 7.75 (7.41). Chracterization of complex **5**: ^{1}H NMR (CD$_2$Cl$_2$, 298 K) 7.60 (d, $^3J_{HH}$ = 2.1, H-3), 7.42 (m, *o*-H), 7.04 (t, $^3J_{HH}$ = 7.4, *m*-H), 6.91 (H-5), 6.90 (t, $^3J_{HH}$ = 7.2, *p*-H), 6.36 (t, $^3J_{HH}$ = 2.5, H-4), 5.13 (d, $^2J_{HH}$ = 14.6, H-1), 4.56 (d, $^2J_{HH}$ = 14.6, H-2), 1.01 (d, $^2J_{PH}$ = 7.9, PMe$_3$), 0.25 (d, $^3J_{PH}$ = 4.7, Me); ^{13}C{^{1}H} NMR 243.4 (d, $^2J_{CP}$ = 9.7 *C*OMe), 199.1 (d, $^2J_{CP}$ = 16.8, CO (cis)), 189.8 (d, $^2J_{CP}$ = 94.9, CO (trans)), 164.3 (q, $^1J_{BC}$ = 48.1, C-ipso), 147.8 (s, C-3), 146.1 (s, C-3′), 137.5 (s, C-5), 136.4 (s, *o*-C), 135.8 (s, C-5′), 126.4 (s, *m*-C), 122.2 (s, *p*-C), 108.9 (s, C-4′), 108.2 (s, C-4), 62.1 (s, CH$_2$), 51.9 (s, CO*M*e), 13.7 (d, $^2J_{CP}$ = 30.3, PMe$_3$); ^{31}P{^{1}H} NMR −17.36 (s); IR (CH$_2$Cl$_2$) ν_{CO} 2042, 1985 cm^{-1}. Characterization of complex **6**: ^{1}H NMR (CD$_2$Cl$_2$, 298 K) 7.57 (s, H-3), 7.42 (m, *o*-H), 7.41 (s, H-3′), 7.15 (d, $^3J_{HH}$ = 2.4, H-5), 7.04 (t, $^3J_{HH}$ = 7.4, *m*-H), 6.98 (d, $^3J_{HH}$ = 2.5, H-5′), 6.90 (t, $^3J_{HH}$ = 7.2, *p*-H), 6.33 (m, H-4), 6.30 (t, $^3J_{HH}$ = 2.5, H-4′), 5.24 (br d, H-1), 5.11 (br d, H-2), 1.61 (d, $^2J_{PH}$ = 10.0, PMe$_3$), 0.04 (d, $^3J_{PH}$ = 4.8, Me); ^{31}P{^{1}H} NMR 12.02 (s); IR (CH$_2$Cl$_2$) ν_{CO} 2047, 1985 cm^{-1}. Chracterization of complex **7**: ^{1}H NMR (CD$_2$-Cl$_2$, 298 K) 4.96 (d, $^2J_{HH}$ = 15.2, H-2), 4.64 (d, $^2J_{HH}$ = 15.2, H-1), 0.92 (d, $^2J_{PH}$ = 9.2, PMe$_3$), 0.20 (d, $^3J_{PH}$ = 6.8, Me).

Preparation of *cis*-[Ru(PMe$_3$)(CO)$_2$(I)(pz$_2$-CH$_2$)]BPh$_4$ (9). The residual solution of the synthesis of complex **4** was still fluxed with CO for 1 h and placed in the refrigerator for 12 h at −18 °C. Complex **9** precipitated as a pale yellow solid. For **9**: ^{1}H NMR (CD$_2$Cl$_2$, 298 K) 7.63 (d, $^3J_{HH}$ = 2.2, H-3), 7.45 (m, *o*-H), 7.02 (t, $^3J_{HH}$ = 7.5, *m*-H), 6.97 (d, $^3J_{HH}$ = 2.8, H-5), 6.86 (t, $^3J_{HH}$ = 7.2, *p*-H), 6.46 (td, $^3J_{HH}$ = 2.6, H-4), 6.33 (d, $^2J_{HH}$ = 14.2, H-2), 4.63 (d, $^2J_{HH}$ = 14.2, H-1), 1.05 (d, $^2J_{PH}$ = 10.5, PMe$_3$); ^{13}C{^{1}H} NMR 195.0 (d, $^2J_{CP}$ = 11.3, CO), 164.6 (q, $^1J_{BC}$ = 49.4, C-ipso), 147.3 (s, C-3), 138.0 (s, C-5), 136.7 (s, *o*-C), 126.8 (s, *m*-C), 123.1 (s, *p*-C), 109.9 (s, C-4), 63.9 (s, CH$_2$), 13.7 (d, $^2J_{CP}$ = 33.8, PMe$_3$); ^{31}P{^{1}H} NMR 10.89 (s); IR (CH$_2$-Cl$_2$) ν_{CO} 2076, 2026 cm^{-1}. Anal. Calcd (found) for (C$_{36}$H$_{37}$N$_4$-BIO$_2$PRu): H, 4.50 (4.46); C, 51.11 (50.87); N, 6.79 (6.68).

X-ray Crystallography. Crystals of **4** suitable for X-ray single-crystal study were grown from ethanol/diethyl ether. Diffraction intensities were collected by the $\theta-2\theta$ scan method on a graphite-monochromated Enraf-Nonius CAD-4 diffractometer and reduced to F_0^2 values. Structure solved by direct methods and refined by full-matrix least-squares calculations. For all computations, SHELXS86[11] and SHELXL93[11] were employed. Thermal vibrations for all non-H atoms were treated anisotropically. All H atoms were found in difference Fourier maps and refined with adequate constraints (C−H = 0.96 Å). Final difference Fourier map showed residual peaks lower than 0.51 e Å^{-3} in the proximity of the Ru atom. Table 4 reports the experimental parameters of data collection and refinement.

(8) Weissberger, A.; Proskauer, E. S. *Technique of Organic Chemistry*; Interscience: New York, 1955; Vol. VII.
(9) (a) Julia, S.; Sala, P.; del Mazo, J.; Sancho, M.; Ochao, C.; Elguero, J.; Fayet, J.-F.; Vertut, M.-C. *J. Heterocycl. Chem.* **1982**, *19*, 1141. (b) Julia, S.; del Mazo, J.; Avila, L.; Elguero, J. *Org. Prep. Proc. Int.* **1984**, *16* (5), 299.
(10) Macchioni, A.; Pregosin, P. S.; Engel, P. F.; Mecking, S.; Pfeffer, M.; Daran, J.-C.; Vaissermann, J. *Organometallics* **1995**, *14*, 1637 and references therein.

(11) Sheldrick, G. M. SHELXS86 *Acta Crystallogr. Sect. A* **1990**, *46*, 467. Sheldrick, G. M. SHELXL93, Program for Crystal Structure Refinement, University of Gottingen, Germany, 1993.

**Table 4.   Crystal Data and Details of
Measurements for 4**

formula	$C_{38}H_{40}BN_4O_3PRu$
mol wt	743.6
temp	293
system	monoclinic
space group	$P2_1/c$
a (Å)	16.595(3)
b (Å)	10.362(3)
c (Å)	21.309(5)
β (deg)	96.41(3)
V (Å^3)	3641(2)
Z	4
$F(000)$	1536
λ (Mo Kα) (Å)	0.71069
μ (Mo Kα) (mm^{-1})	0.52
ϑ range (deg)	2.5–25
octants explored	$\pm h, +k, +l$
measd reflns	6584
unique reflns used in the refinement	6393
no. of refined params	504
GOF on F^2	0.926
R_1 (on F, $I > 2\sigma(I)$)	0.049
wR$_2$ (on F^2)	0.145

Calculations. The molecular models were performed using the Sybyl[12] and Spartan[13] packages. The initial structures were built starting from the X-ray crystallographic coordinates. Energy minimization was not performed on the structures.

Simulation of molecular interaction was carried out using the DOCK command[14,15] provided by the Sybyl package, which permits a real-time approximation of the total intermolecular energy of all possible nonbonded interactions between pairs of molecules. More precisely, the total interaction energy is given by $E_{tot} = \Sigma(E_Q + E_{LJ})$ where E_Q is the electrostatic contribution to the interaction energy of each atom i of one molecule interacting with all the j atoms of the other molecule, and where E_{LJ} are the steric attractive and repulsive contributions of each atom i of one molecule interacting with all the j atoms of the other molecule. The analytical dissection of E_Q and E_{LJ} into parameters and mathematical formulas may be found elsewhere.[14,15] The atomic charges for the two molecular structures were obtained using the AMI−SM2 nonpolar solvent calculation and the 3-21G* ab initio models implemented in Spartan. Since the atomic charges were similar, the latter method was selected for the docking. In the docking between the two molecules, positive energies highlight repulsive interactions, while negative energies along with their locations delineate regions of attraction between the two interacting molecules.

Supporting Information Available: Atomic coordinates and equivalent isotropic displacement parameters (Table S1), all bond lengths and angles (Table S2), anisotropic displacement parameters (Table S3), and H-atom coordinates and isotropic displacement parameters (Table S4) for **4** (8 pages). Ordering information is given on any current masthead page.

(12) Sybyl Molecular Modeling Software, version 6.3, TRIPOS Inc. 1699, Manley Road, St. Louis, MI.

(13) Spartan Software, Wavefunction Inc., 18401 V. Karman Avenue, Suite 370, IRVINE, CA 92612.

(14) Clark, M.; Cramer, R. D., II; Van Opdenbosh, N. *J. Comput. Chem.* **1989**, *10*, 982.

(15) Vinter, J. G.; Davis, A.; Sanders, M. R. *J. Comput.-Aided Mol. Des.* **1987**, *1*, 31.